REPRESENTATION OF EARTHQUAKE EFFECTS IN DESIGN ROUTINE

El-Sayad A. Mashaly and Essam A. Elkordi
Structural Engineering Department,Faculty of Engineering
Alexandria University, Alexandria, Egypt.

ABSTRACT

In design routine work of structures, earthquake effects can be taken into consideration by several methods. One of these methods is the static lateral load procedure. An investigation of the lateral load patterns which represent the effects of earthquake excitations introduced by different codes as well as other proposed patterns are studied in this paper. Five buildings are used to conduct this analysis. One of them is designed specifically for this investigation. Four real earthquake records are used to examine failure pattern for each building. A comparison between the actual dynamic failure pattern and the kinematic mechanism of each static lateral load pattern investigated in this study is conducted. The study concludes that the lateral load pattern proportional to the masses gives the best approximation to the actual mode of failure.

Keyword: Structural analysis, Earthquake response analysis, Code provision.

INTRODUCTION

Egyptian Code of Practice and Design of Reinforced Concrete Structures of 1989 (ECPD) [1] requires that buildings should be designed to resist seismic forces in the routine work. A static lateral load representing the effects of expected earthquake excitation at the site should be applied simultaneously along with gravity loads. The ECPD considers this static lateral load as a triangular pattern in addition to a concentrated force at the roof level. Nevertheless, the idea of that pattern is to predict the dynamic response at failure [2]. The static lateral load pattern attempts to predict the dynamic mechanism and does not represent the effective dynamic load at any particular instant. That is because the effective dynamic load pattern is varying continuously during the dynamic response. Although a particular kinematic mechanism is associated with a certain range of lateral load distributions, it may vary significantly for different load distributions depending on the properties of the structure. The importance of identifying the failure pattern is that the shear capacity of the structure can vary significantly from one pattern to another. In identifying the load pattern which leads to better predictions of the failure mode, a group of static lateral load patterns is examined.

LATERAL LOAD PATTERN

Four lateral load pattern are considered in the present study;

1- The Lateral Load Pattern of the ECPD of 1989 [1]; i.e, a triangular lateral load pattern in addition to a concentrated load at the roof.
2- Lateral Load Pattern Proportional to the Masses; where, a lateral load pattern proportional to the masses is considered in this study. For regular buildings, the masses of all floors are reasonably uniform including the roof although its mass is little less than the rest of floors.
3- The Seismic Provisions of the National Earthquake Hazards Reduction Program NEHRP [3] in which the lateral seismic force F_x induced at any level is obtained using the following formula:

$$F_x = C_{vx} V_x \tag{1}$$

where

$$C_{vx}=W_x h^k_x / \sum_{i=1}^{n} W_i h^k{}_H \qquad (2)$$

where V_x is the total base shear. W_i and W_x are the portions of W located at or assigned to level i and x respectively. h_i and h_x are the heights above the base to level i and x; and k is a parameter accounts for the effect of higher modes on the profile of the lateral seismic forces. k is equal to 1 for buildings having a period of 0.5 or less and equal to 2 for buildings having a period of 2.5 seconds or more. For buildings having a period between 0.5 and 2.5 seconds, k may be taken as 2 or may be determined by linear interpolation between 1 and 2.

4- A Lateral Load Pattern Based on the Estimate of Maximum Elastic Base Shear.

In the investigation of the kinematic mechanism that controls the dynamic response, it is reasonable to examine a lateral load pattern which is a function of the structural and ground motion characteristics. In an attempt to develop a procedure defining the lateral load pattern that reflects the structural as well as the ground motion characteristics, it was assumed that the distribution of the lateral load corresponding to the maximum base shear is a reasonable pattern for predicting the actual mechanism of a building. The square root of sum of the squares (SRSS) of the modal contributions gives a reasonable estimate for the maximum base shear [4]. Although the SRSS can be calculated by combining the contributions of all degrees of freedom involved in the structural modeling, the first and the second modes usually contribute the most [4]. Thus, they are considered in the calculation of the base shear. The SRSS of the base shear can be written as the summation of two fractions of the base shears contributed by the first and the second modes as :

$$V_{(SRSS)}=\alpha_1 V_1+\alpha_2 V_2 \qquad (3)$$

where V_1 and V_2 are the peak amplitude modal base shear contributions of the first and second modes, respectively. α_1 and α_2 are the fractions of their amplitudes when the base shear reaches its peak. Because the effect of gravity on the elastic behavior is minimal [4], a first order analysis is employed in the following calculation of the base shear. Using the spectral approach, V_1 and V_2 can be determined as:

$$V_1=\{r\}^T S_{a1}\Gamma_1[M]\{\phi_1\}\ ,\ V_2=\{r\}^T S_{a1}\Gamma_1[M]\{\phi_1\} \qquad (4)$$

where S_{a1} and S_{a2} are the acceleration response spectral ordinates for the first and second natural period of the structure respectively. Γ_1 and Γ_2 are the participation factors associated with first and second modes, $\{\phi_1\}$ and $\{\phi_2\}$ respectively, where Γ_i is expressed as:

$$\Gamma_i=\frac{\{\phi_i\}^T[M]\{r\}}{\{\phi_i\}^T[M]\{\phi_i\}} \qquad (5)$$

where {r} is the pseudo-static deformation vector (equal {1} for horizontal ground excitation).

To determine values for α's, a value for α_1 can be estimated based on the expected contribution of the first mode to the value of maximum base shear and then, solve for α_2 as

$$\alpha_2=\frac{V_{(SRSS)}-\alpha_1 V_1}{V_2} \qquad (6)$$

Although the theoretical range of the values of α_1 varies from an upper bound of 1.0 to a lower bound which can be determined by setting α_2 equal to 1.0, the actual values of α's can be obtained by performing time-history analysis using two SDOF systems. The first system has a natural period equal to first natural period of the real building and a damping ratio equal to the damping ratio associated with the building's first mode. The second system has a natural period equal to the second natural period of the same building and a damping ratio equal to the damping ratio associated with the building's second mode. The generalized displacements Y_1 and Y_2 of both systems can be determined at each time step. Substituting into Eq.(4) using $Y_1\,\omega^2$ and $Y_2\,\omega^2$ instead of S_{a1} and S_{a2}, the base shear associated with each system can be calculated at each time step. Adding these two values of the base shear at each time step, the maximum value of the base shear and the associated values of V_1 and V_2 can be determined. Once V_1 and V_2 are determined, the corresponding generalized displacements of both systems, Y_1 and Y_2, can also be obtained. Knowing the maximum generalized displacements Y_{m1} and Y_{m2} during the entire response, the α's can be determined as:

$$\alpha_1 = Y_1/Y_{m1} \quad , \quad \alpha_2 = Y_2/Y_{m2} \tag{7}$$

The ten-story one bay frame shown in Figure (2) is selected to examine the variation of the values of α_2 and to determine values that can be used for the calculation of the load pattern. In the calculation of its corresponding two SDOF system, the damping ratios associated with the first and the second modes are selected as 5% of the critical. The values of α_1 and their associated values of α's are calculated for four ground motions; namely ELC, TAF, PAC and IVC. these values are listed in Table (1).

During the course of this analysis, it was recognized that since the maximum base shear is a combination of the values of V_1 and V_2 at a certain time step, there might be a chance that more than one combination at different time steps can lead to the same value of the maximum base shear. Thus, in the evaluation of α's there might be a range for their values instead of certain values. Table (2) shows also these ranges of α_1 associated with 5% range of the maximum base shear for the four ground motions. As can be seen, the values of α_1 is ranging between 0.95 and 1.0 in the case of ELC, and between 0.69 and 1.0 in the case of IVC. To examine the significance of the variations in α_1 on the associated load pattern and then the effect of the resulting load pattern on the predicted mechanism, values for α_1 equal to 1.0, 0.95, and 0.90 are selected. Investigation of the variation of the lateral load patterns associated with these three values of α_1 with respect to each other for the four ground motions shows that the load pattern can vary significantly. However, examining the effect of the variation in the load pattern does not necessarily lead to a change in the kinematic mechanism.

As mentioned earlier, each mechanism shape is associated with a certain range of lateral load distributions. It should be emphasized that the critical aspect is the variation in the mechanism shape and not in the load pattern. Based on this study, it was found that there is no a single value of α_1 can always lead to the actual dynamic mechanism and thus, a value for α_1 equal to 0.95 is determined to be the best among the three investigated values which might lead to the actual dynamic mechanisms. For this reason,α_1 equal to 0.95 is considered for the rest of the study.

Once α_1 and α_2 are determined, the lateral load pattern can be calculated as:

$$\{L\} = \alpha_1\{L_1\} + \alpha_2\{L_2\} \tag{8}$$

where $\{L_1\}$ and $\{L_2\}$ are the modal load vectors that can be calculated as:

$$\{L_1\} = S_{a1}\Gamma_1[M]\{\phi_1\} \ , \ \{L_2\} = S_{a2}\Gamma_2[M]\{\phi_2\} \tag{9}$$

It should be mentioned that lateral load pattern $\{L\}$, calculated from Eq.(8) represents the relative distribution of the lateral load at each level and can be scaled to any appropriate factor for the purpose of the calculation of the mechanism capacity.

EXAMINED BUILDINGS

Five buildings are examined in this research. The first building is an eight-story five-bay building designed according to the 1970 ECPD [11] code shown in Figure (1). This building was presented by Abdelrahman *et al.* [12]. The fundamental natural period is 1.0 second. The second is a ten-story one-bay building presented by Anderson and Betrero [7], shown in Figure (2). The building was designed in accordance with the 1967 UBC code [13]. The fundamental natural period of this frame is 2.2 seconds. The third one is a ten-story three-bay building also presented by Anderson and Bertero [8], shown in Figure (3). This building was designed in accordance with the 1982 UBC code [10]. The fundamental natural period is 2.11 seconds. A twelve-story one-bay building presented by Assaf [9] is chosen as the fourth building, shown in Figure (4). This building was designed in accordance with the 1988 NEHRP Code [3] and then the strength of the columns was modified by Assaf in such a way that the building is forced to fail globally. The Fundamental natural period of this frame is 1.89 seconds. The Fifth building is twelve-story five-bay building designed specifically for this study according to the ECPD code of 1989 [1], shown in Figure (5). The fundamental natural period is 1.4 seconds.

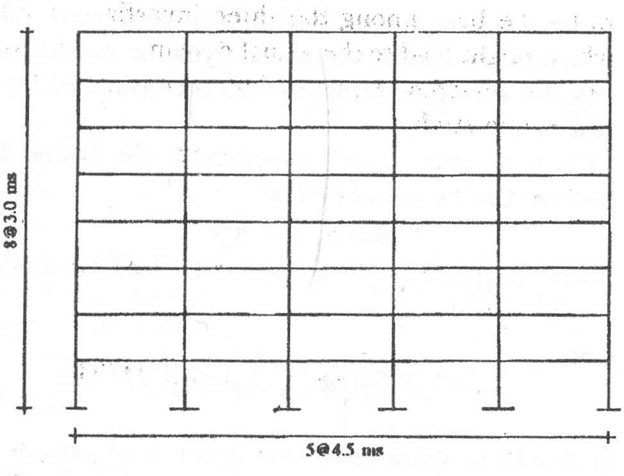

Figure 1. Eight-story five bay frame.

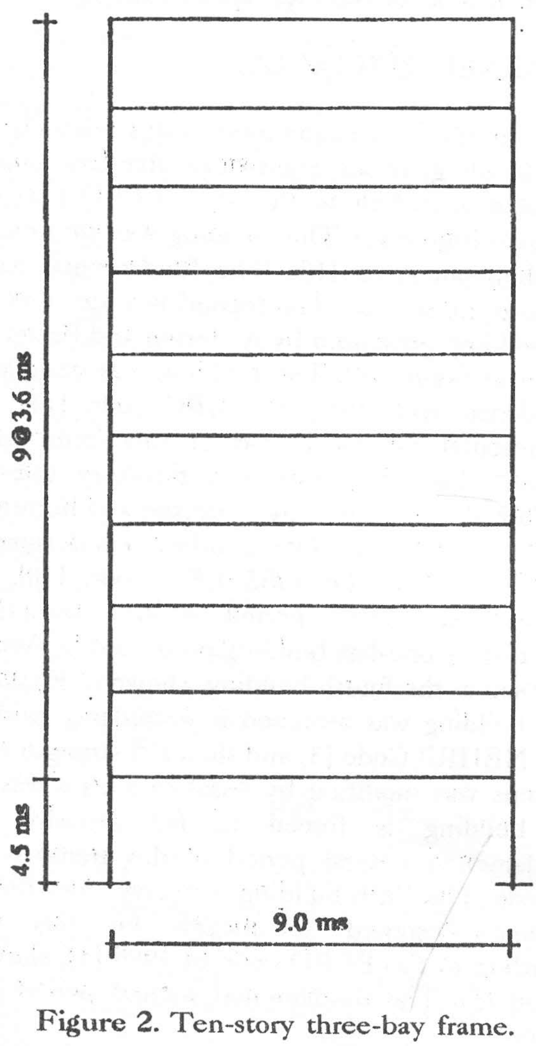

Figure 2. Ten-story three-bay frame.

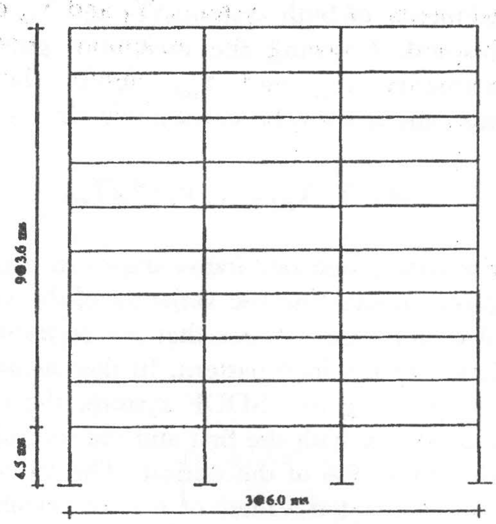

Figure 3. Ten-story three-bay frame.

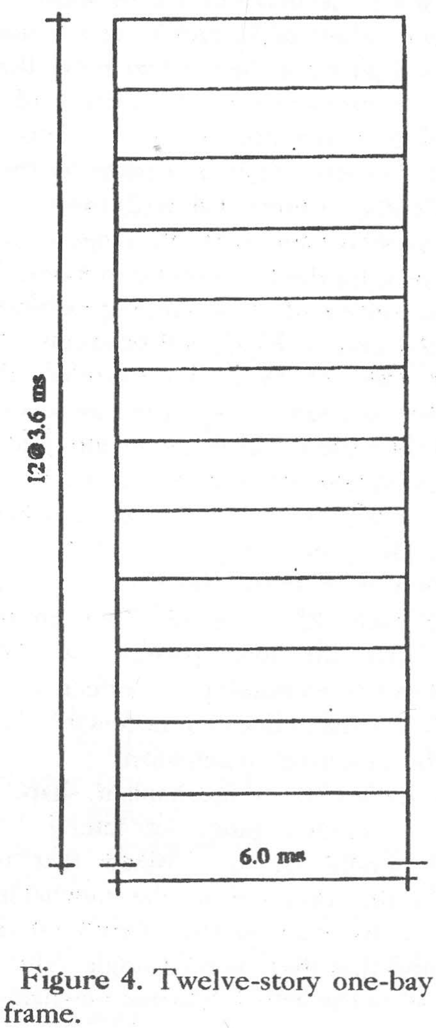

Figure 4. Twelve-story one-bay frame.

Table 1 Earthquake Characteristics

Earthquake Record	Date of Earthquake	Peak Ground Motions			Complete Duration (sec)
		Acc. (g)	Vel. (in/sec)	Dis. (in)	
El Centro (ELC) S00E Comp	5/18/1940	0.348	13.15	4.88	55.76
Taft (TAF) S69E Comp.	7/21/1952	0.179	6.97	4.13	55.76
Imperial Valley College (IVC) S50W Comp	10/15/1979	0.462	42.44	16.93	37.70
Pacoima Dam (PAC) S16E Comp	2/09/1971	1.170	44.57	16.50	46.32

Table 2 Values of α_1 and α_2 for Ten-Story One-Bay Frame

Earthquake	α_1 (%)	α_2 (%)	Range of α_1 (%) within 5% of Max. Base Shear
ELC	98.1	71.0	100 – 95
PAC	92.1	7.2	100 – 77
IVC	79.8	55.2	100 – 69
TAF	97.7	64.5	100 – 90

ANALYSIS OF RESULTS

The lateral load patterns presented in this study are examined in order to determine which pattern leads to a better prediction of the critical dynamic mechanism. The five presented buildings are used in this examinations. The actual dynamic mechanism of each building is computed for four ground motion excitations (ELC, TAF, PAC, and IVC) by performing non-linear dynamic analysis [5] after scaling each ground motion record by the factor which leads to the buildings failure. The critical dynamic mechanism is identified by tracing the incremental displacement shape during the different stages of response until there is a large deformation of the building. The kinematic mechanism of each building is computed by performing non-linear static analysis [5]. The pattern of each lateral load is kept constant and its magnitude is increased monotonically until the mechanism occurs. The kinematic mechanism is identified by tracing the plastic hinges until the formation of the mechanism.

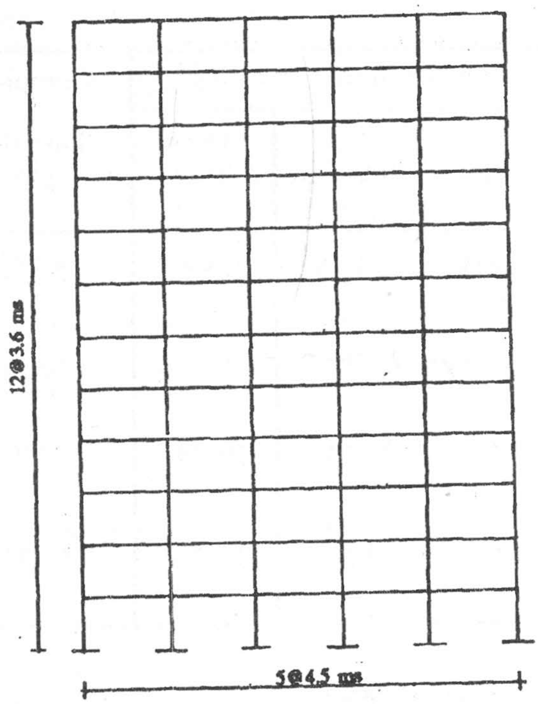

Figure 5. Twelve-story five-bay frame.

The dynamic mechanism as well as the kinematic mechanism associated with the static load patterns are shown in Figures (6) to (10). As can be seen, for four buildings, their dynamic mechanisms were local and for the fifth one it was global. It should be mentioned that the building with global mechanism (the twelve-story one-bay frame) was forced to fail globally by providing large strength for the columns. Therefore, the four cases of this building will be excluded from the total number of cases in the evaluation of the patterns. With regard to the prediction of the dynamic mechanism for the remaining 16 cases of the other four buildings, the results indicate the following:

(1) The ECPD lateral load pattern predicted the critical dynamic mechanism correctly in 6 cases, the predicted mechanism was close to the actual one in 6 cases and was far off the actual mechanism in 4 cases.

(2) The lateral load pattern proportional to the masses predicted the critical dynamic mechanism correctly in 14 cases, the predicted mechanism was close to the actual one in the remaining 2 cases.

(3) The NEHRP-load pattern predicted the critical dynamic mechanism close to the actual one in 9 cases and was far off the actual mechanism in 7 cases.

(4) The SRSS-lateral load pattern predicted the critical dynamic mechanism correctly in 10 cases, the predicted mechanism was close to the actual one in 6 cases.

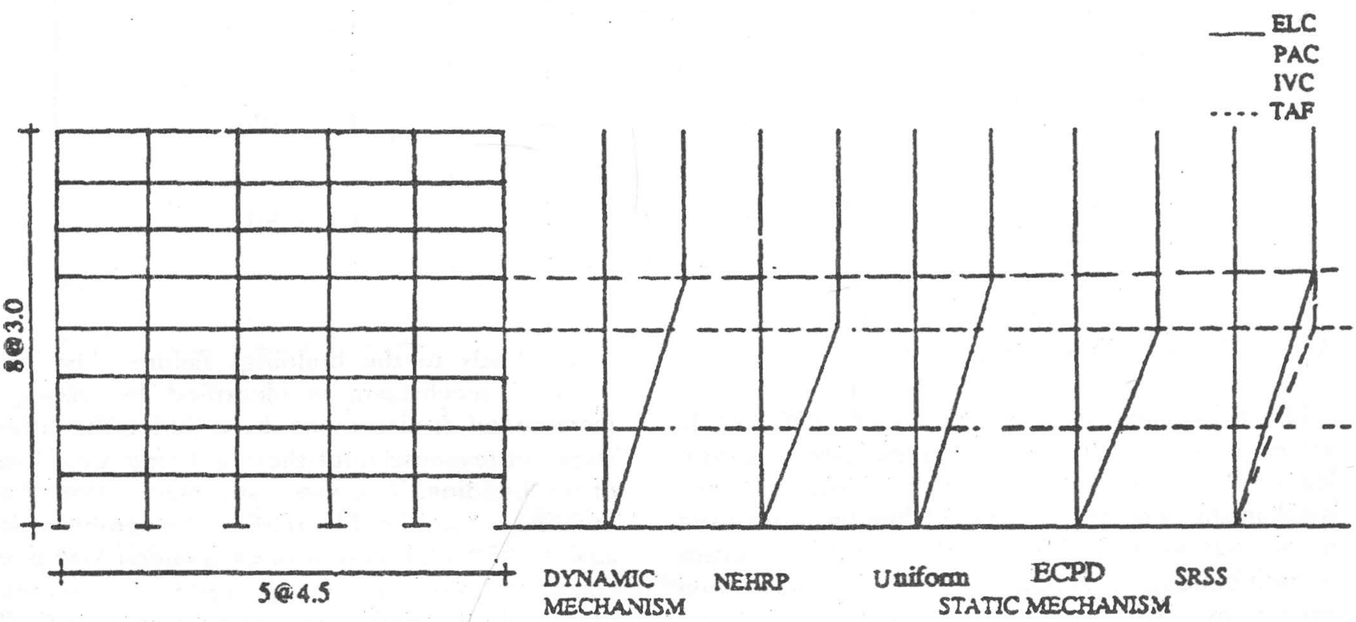

Figure 6. Comparison between dynamic mechanism and kinematic mechanisms.

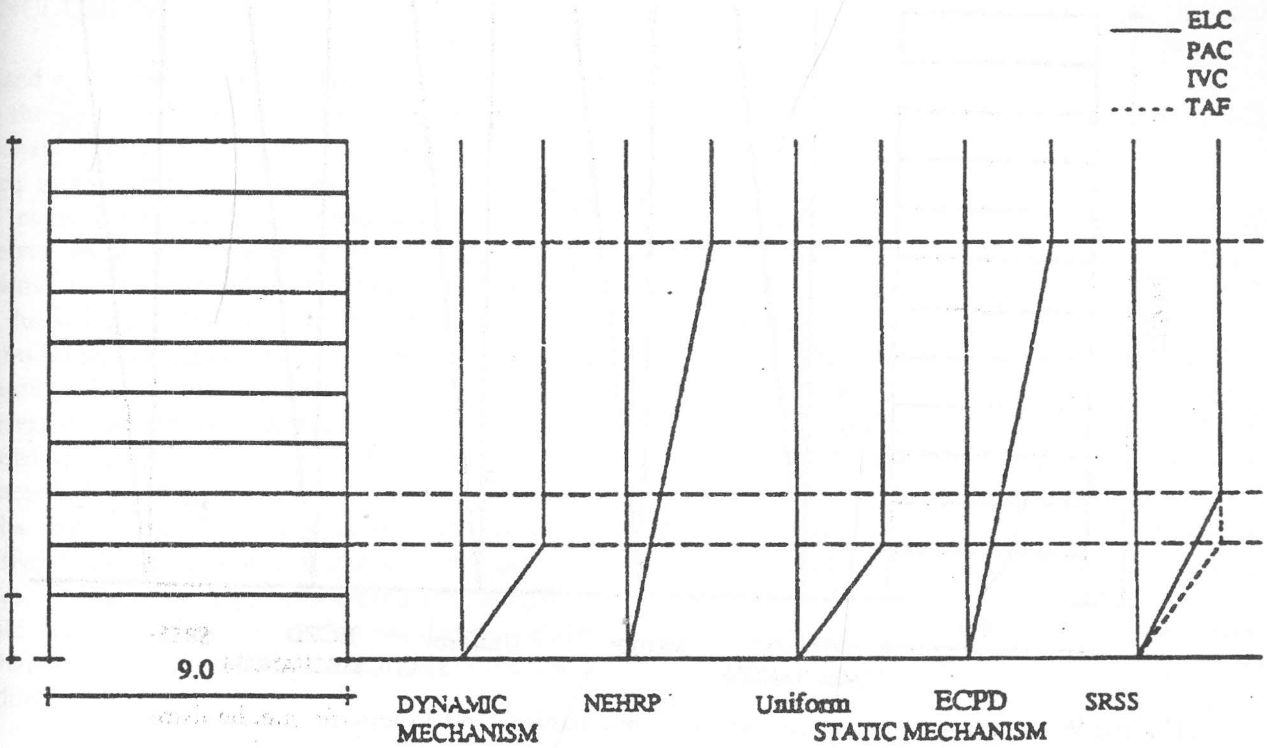

Figure 7. Comparison between dynamic mechanism and kinematic mechanisms.

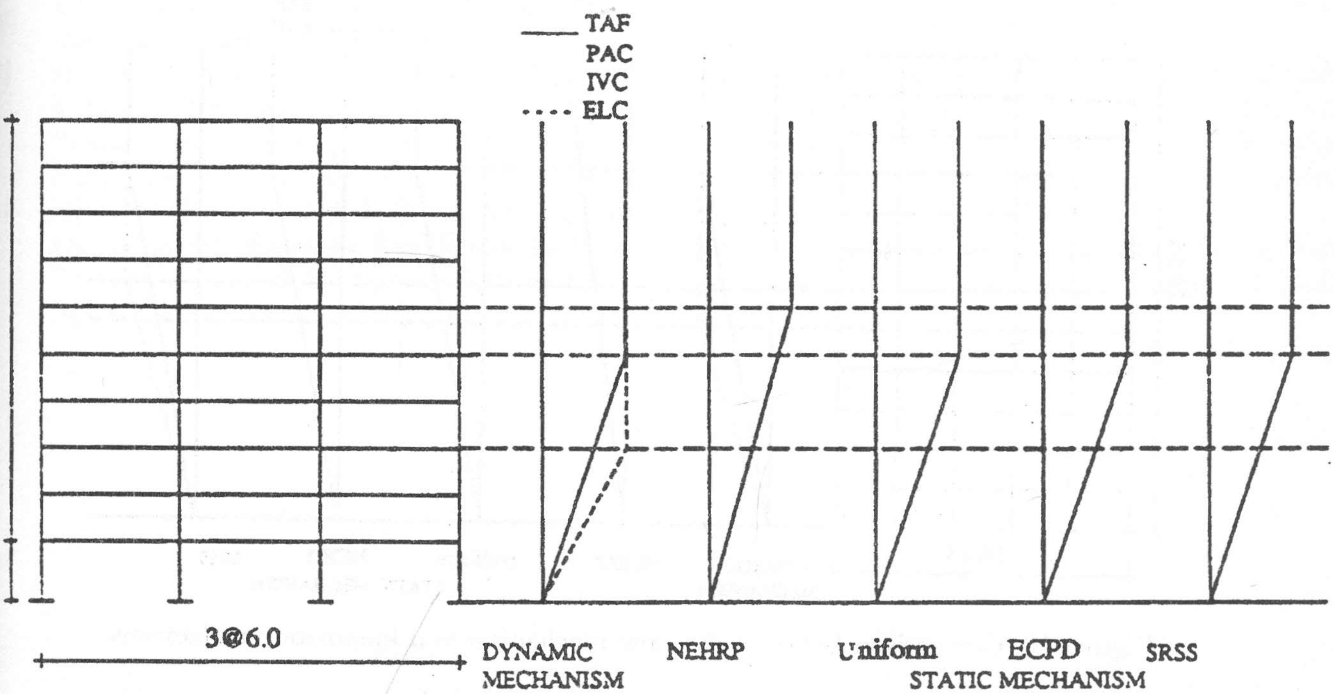

Figure 8. Comparison between dynamic mechanism and kinematic mechanisms.

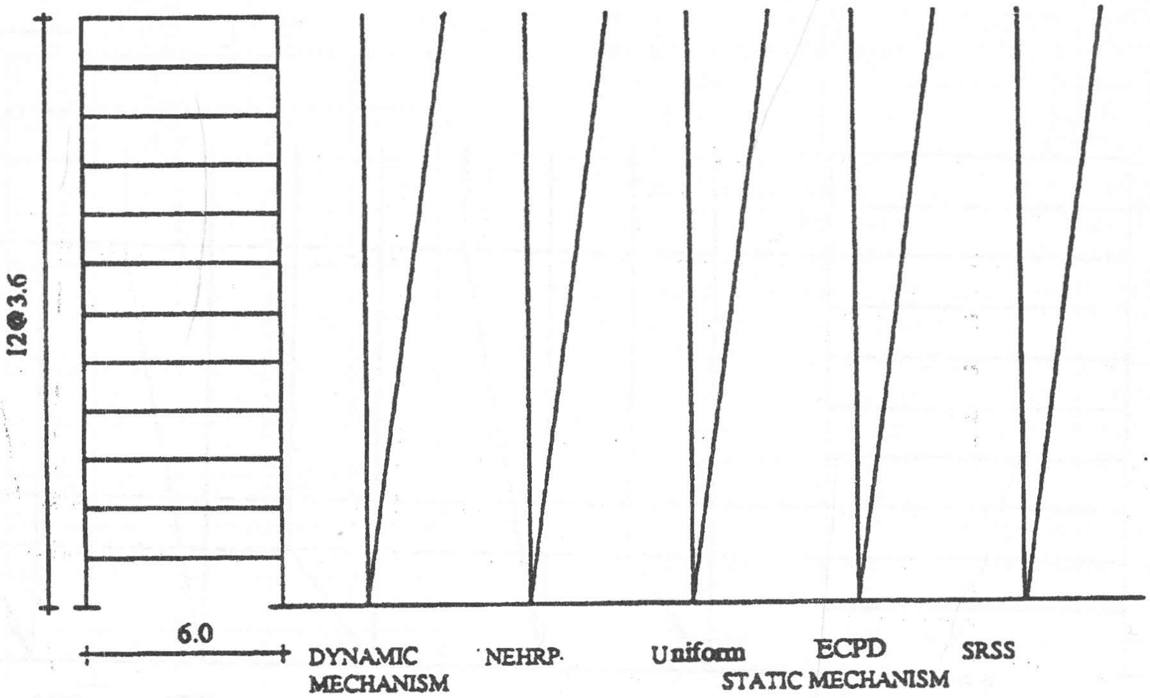

Figure 9. Comparison between dynamics mechanism and kinematic mechanisms.

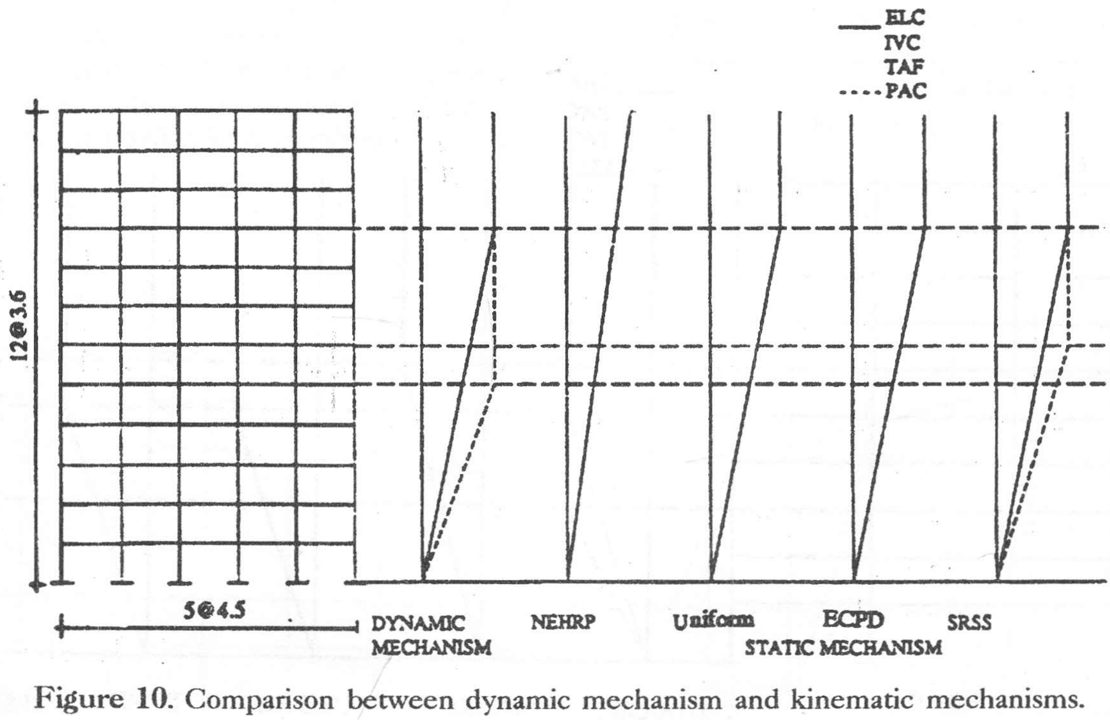

Figure 10. Comparison between dynamic mechanism and kinematic mechanisms.

CONCLUSION

Based on the preceding results, it can be concluded that the uniform lateral load pattern appears to be a reasonable choice as the static lateral load pattern which gives better predictions for the mechanisms that control the dynamic responses. It was also observed from the dynamic analyses that the actual dynamic mechanism of each investigated building was the same for all four ground motions except for two buildings; one ground motion gave a mechanism different from the other three. From this observation, it appears that the actual mechanism is somewhat independent of the ground motion characteristics. It can also be observed from the results that non of the design codes used to design the five buildings insured a global mechanism for failure. Therefore, it is recommended that provisions should be provided in codes to insure global mechanism in order to increase the shear capacity of buildings.

REFERENCES

[1] Ministry of New Society and Housing, "The Egyptian Code of Practice and Design of R.C. Structures" Cairo, Egypt 1989.

[2] H. Takizawa and P.C. Jennings, "Collapse of a Model for Ductile Reinforced Concrete Frames under Extreme Earthquake Motions" *Earthquake Eng. and Struct. Dyn.*, vol. 8, 1980.

[3] NEHRP Recommended Provisions for the Development of Seismic Regulations for New Buildings, Federal Emergency Management Agency, 1988 Edition FEMA, 1988.

[4] R.W. Clough and J. Penzien, *Dynamic of Structural Analysis*, Thomas Nelson & Sons Ltd 1980.

[5] V. Prakash and G.H. Powell, "DRAIN-2DX", User Guide, University of California, Berkely, USA, 1992.

[6] S.L. Wood, R. Strak and S.A. Greer, "Collapse of Eight-Story R.C. Building During 1985 Chile Earthquake," *Journal of Structural Eng.* vol. 117, No.2, Feb. 1991.

[7] J.C. Anderson and V.V. Bertero, "Seismic Behavior of Multi-story Frames Designed by Different Philosophies" Report No. EERC69-11, earthquake Engineering Research Center, University of California at Berkely, Oct. 1969.

[8] J.C. Anderson and V.V. Bertero, "Uncertainties in Establishing Design Earthquakes" *J. Struct. Div., ASCE*, vol. 113, No.8, 1987.

[9] A.F. Assaf, "Evaluation of the Structure Overstrength of Steel Building Systems" Master Thesis, Dept. of Civil Eng., Northeastern University, Boston, Mass., 1989.

[10] Uniform Building Code (UBC), Int. Conf. of Building Officials, Whittier California, 1988.

[11] Ministry of Scientific Research, "The Egyptian Code of Practice and Design of R.C. Structures" Cairo, Egypt 1970.

[12] A. Abdel-Rahman, A. Maaruof and E. Elkordi, "Seismic Problem From Adding New Floors to Old Buildings in Egypt" Second Alexandria Conference on Structural and Geotechnical Eng., April 1994.

[13] Ministry of Scientific Research, "The Egyptian Code of Practice and Design of R.C. Structures" Cairo, Egypt 1967.